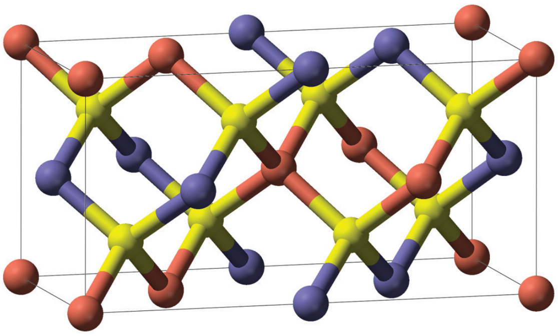

Figure 13.19: The crystal structure of *copper indium diselenide*, a typical chalcopyrite. The colors indicate copper (red), selenium (yellow) and indium (blue). For *copper gallium diselenide*, the In atoms are replaced by Ga atoms [78].

up to several centimetres in growth direction and up to several millimetres orthogonal to the growth direction. These large grains lead to open-circuit voltages comparable to that of wafer-based Si solar cells with reported maximum values of 656 mV [75] and efficiencies of 11.8% have been demonstrated [76].

The highest efficiencies are reached with silicon layers grown in an epitaxy process, just as for the high-performance III-V solar cells. The epitaxy films then are transferred on glass. The current record cell made with this method has an efficiency of 20.1% on a 43 µm thick substrate and was fabricated by the American company SOLEXEL [77].

13.4 Chalcogenide solar cells

The third class of thin-film solar cells that we discuss are the large class of *chalcogenide solar cells*, where our focus mainly will be on CIGS and cadmium telluride (CdTe) solar cells. The term *chalcogenides* refers to all chemical compounds consisting of at least one *chalcogen* anion from the group 16 (also known as *group VI*) with at least one or more electropositive elements. Five elements belong to group 16: oxygen (O), sulphur (S), selenium (Se), tellurium (Te), and the radioactive polonium (Po). Typically, oxides are not included in discussions of chalcogenides. Because of its radioactivity, compounds with Po are of only very limited relevance for semiconductor physics.

13.4.1 Chalcopyrite solar cells

The first group of chalcogenide solar cells that we discuss are *chalcopyrite solar cells*. The name of this class of materials is based on *chalcopyrite* (copper iron disulphide, $CuFeS_2$). Like all the chalcopyrites, its forms *tetragonal* crystals, as illustrated in Fig. 13.19.

Many chalcopyrites are semiconductors. As they consist of elements from groups I, III, and VI, they are also called I-III-VI semiconductors or *ternary* semiconductors. In principle,

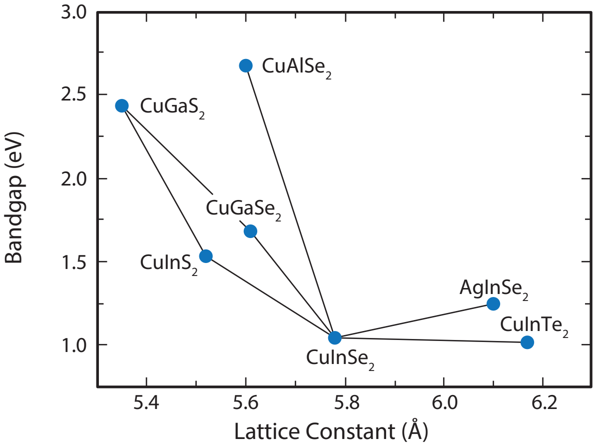

Figure 13.20: The bandgap vs. the lattice constant for several chalcopyrite materials. Data taken from [79].

all these combinations can be used:

$$\begin{pmatrix}\text{Cu}\\\text{Ag}\\\text{Au}\end{pmatrix}\begin{pmatrix}\text{Al}\\\text{Ga}\\\text{In}\end{pmatrix}\begin{pmatrix}\text{S}\\\text{Se}\\\text{Te}\end{pmatrix}_2$$

Figure 13.20 shows the bandgap vs. the lattice structure for several chalcopyrite materials.

The most common chalcopyrite used for solar cells is a mixture *copper indium diselenide* ($CuInSe_2$, CIS) and copper gallium diselenide ($CuGaSe_2$, CGS). This mixture is called *copper indium gallium diselenide* [$Cu(In_xGa_{1\text{-}x})Se_2$, CIGS], where the x can vary between 0 and 1. Several research groups and companies use a compound that also contains sulfur; it is called *copper indium gallium diselenide/disulfide* [$Cu(In_xGa_{1\text{-}x})(Se_yS_{1\text{-}y})_2$, CIGSS], where y is a number in between 0 and 1.

The physical properties of CIGS(S) are rather complex and many different views exist on these properties among scientists. $CuInSe_2$ has a bandgap of 1.0 eV, the bandgap of $CuInS_2$ is 1.5 eV and $CuGaSe_2$ has a bandgap of 1.7 eV. By tuning the In:Ga ratio x and the Se:S ratio y, the bandgap of CIGS can be tuned from 1.0 eV to 1.7 eV. As CIGS(S) is a a direct bandgap semiconductor material, it has a large absorption coefficient, hence an absorber thickness of 1-2 µm is sufficient for absorbing a large fraction of the light with energies above the bandgap energy. Also the typical electron diffusion length is the order of a few micrometers. CIGS(S) is a p-type semiconductor, the p-type character resulting from intrinsic defects in the material that amongst others are related to Cu deficiencies. The many different types of defects in CIGS(S) and their properties are a topic of ongoing research.

Figure 13.21 (a) illustrates a typical CIGS solar cell structure deposited on glass, which acts as a substrate. On top of the glass a *molybdenum layer* (Mo) of typically 500 nm thick is deposited, which acts as the electric back contact. Then, the p-type CIGS absorber layer is deposited with a thickness up to 2 µm. Onto the p-CIGS layer, a thin n-CIGS layer is

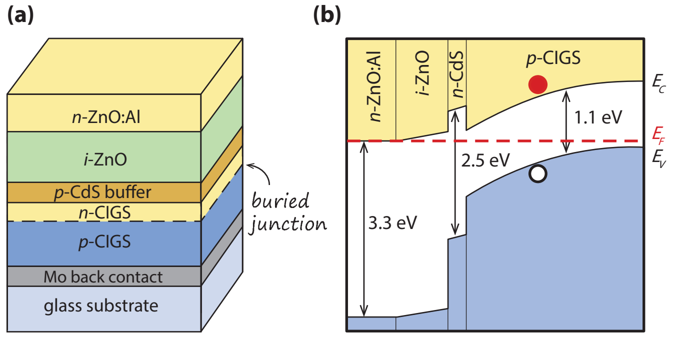

Figure 13.21: The (a) layer structure and (b) band diagram of a typical CIGS solar cell.

deposited, for example an indium/gallium rich $Cu(In_xGa_{1\text{-}x})_3Se_5$ alloy. The *pn*-junction is formed by stacking a thin *cadmium sulphide* (CdS) *buffer layer* of around 50 nm thickness onto the CIGS layers. The *n*-type region is extended with the TCO layer, that also is of *n* type: First an intrinsic *zinc oxide* (ZnO) layer deposited followed by a layer of Al doped ZnO. The Al is used as an *n* dopant for the ZnO. Similar to thin film silicon technology, the *n*-type TCO acts as the transparent front contact for the solar cell.

Figure 13.21 (b) shows the electronic band diagram of a CIGS solar cell. The light enters the cell from the left, via the ZnO. The *p*-type CIGS absorber layers used in industrial modules typically has a bandgap of 1.1-1.2 eV, which is achieved using $Cu(In_xGa_{1\text{-}x})Se_2$ with $x \approx 0.3$ [80]. The *n*-type CdS buffer layer has a bandgap of 2.5 eV. The bandgaps of the *n*- and *p*-type materials are different, which means that such CIGS cells can be considered as heterojunctions. The bandgap of ZnO is very large with values of 3.2 eV or even higher, which minimises the parasitic absorption losses in this device [81].

The defect density at the surface is higher than in the bulk, which could be a loss mechanism for the minority charge carriers. This recombination can be reduced by placing an *n*-type CIGS layer between the *p*-type CIGS and the *n*-type CdS layers, as already mentioned above. The *pn*-junction within the CIGS is called a *buried junction*; there the electron-hole pairs are separated. In *p*-CIGS, which is Cu-deficient, the dominant recombination mechanism is Shockley-Read-Hall recombination in the bulk. In contrast, in Cu rich CIGS films the SRH recombination at the CIGS/CdS interface becomes dominant.

A very important issue in the development of CIGS solar cells is the role of *sodium* (Na). A low contamination with sodium appears to reduce the recombination in *p*-type CIGS materials because of better recombination of the grain boundaries. The reduced recombination rate results in a higher bandgap utilisation and thus a higher open circuit voltages. Typically, the optimal concentration of sodium in the CIGS layers is about 0.1%. Often, as a Na source soda-lime glass is used, that is also the substrate for the solar cell. If no soda-lime glass is used, the Na has to be intentionally added during the deposition process. The scientific question why Na significantly improves several properties of the CIGS films is still not completely solved. Currently, also the influence of *potassium* (K) is heavily investigated.

Fabrication of CIGS solar cells

CIGS films can be deposited with various different technologies. Because many of these activities are developed within companies, not much detailed information is available on many of these processing techniques. One approach is co-evaporation under vacuum condition. Using various crucibles of copper, gallium, indium and selenium, the precursors are co-evaporated onto a heated substrate. The second approach is sputtering onto a substrate at room temperature. After that, the substrate is *thermally annealed* under presence of selenium vapour, such that the CIGS structure can be formed. Alternatively, a selenium rich layer can be deposited on top of the initially deposited alloy, followed by an annealing step. Because of the variety and complexity of the reactions taking place during the *'selenisation'* process, the properties of CIGS are difficult to control. Companies that use or have used co-evaporation process are Würth Solar, Global Solar and Ascent Solar Technologies. Among CIGS companies using sputter approaches are Solar Frontier, Avancis, MiaSolé and Honda Soltec.

An alternative approach to produce CIGS layers is based on a *wafer bonding* technique. Two different films are deposited onto a substrate and a superstrate, repspectively. Then, the films are pressed together on high pressure. During annealing, the film is released from the superstrate and a CIGS film remains on a substrate.

Non-vacuum techniques can be based on depositing nanoparticles of the precursor materials on a substrate after which the film is sintered. During the *sintering process* films are made out of powder. For achieving this, the powder is heated up to a temperature below the melting point. At such high temperatures, atoms in the particles can diffuse across the particle boundaries. The particles thus fuse together forming one solid. This process has to be followed by a *selenisation step*.

An important advantage of the CIGS PV technology is that on it has achieved the highest conversion efficiencies among the different thin-film techologies except the III-V technology. The current record for lab-scale CIGS solar cells processed on glass is 20.8% and was achieved by the German research institute ZSW [47]. This record cell has a V_{oc} of 0.757 V, a J_{sc} of 34.77 mA/cm^2, and a FF of 79.2%. The world record on flexible substrates has been obtained at the Swiss Federal Laboratories for Materials Science and Technology (EMPA). On flexible polymer foil they achieved a conversion efficiency of 20.4% [82].

For making CIGS modules, the interconnection is done as discussed in detail in Chapter 15. As generally true for the different PV technologies, the record efficiencies of modules are significantly lower than that of lab-scale cells. The record efficiencies of 1 m^2 modules are in the order of 13%, whereas the aperture-area efficiencies are just above 14% as confirmed by NREL. The German manufacturer Manz AG has presented an 15.9% aperture area efficiency and a total area efficiency of 14.6%. The Japanese company Solar Frontier claims a 17.8% aperture area efficiency on a small module of 900 cm^2 size.

Despite the very high conversion efficiencies, the CIGS technology faces several challenges. As CIGS is a deposited in a complex deposition processes, it is challenging to perform large area deposition with a high *production yield*, *i.e.* the percentage of all the modules coming out of the production line that fulfil the product specifications.

Kesterites

Figure 13.1 shows the abundance in the Earth's crust for several elements. As we can see, indium is a very rare element. However, it is a crucial element of CIGS solar cells. Because of its scarcity, In might be *the* limiting step in the upscaling of the CIGS PV technology to future terawatt scales. In addition, the current thin-film display industry depends on In as well, as ITO is integrated in many display screens.

As a consequence, other chalcogenic semiconductors are investigated that do not contain rare elements. A interesting class of materials are the *kesterites* which are *quarternary* or *pentary* semiconductors consisting of four or five elements, respectively. While the name giving mineral kesterite [$Cu_2(ZnFe)SnS_4$], where zinc and iron atoms can substitute each other, is not used as a semiconductor, kesterite without iron (Cu_2ZnSnS_4) is used. It also is known as *copper zinc tin sulphide* (CZTS) and is a I_2-II-IV-VI_4 semiconductor. Other kesterites are for example *copper zinc tin selenide* ($Cu_2ZnSnSe_4$, CZTSe), or ones using a mixture of sulphur and selenium, $Cu_2ZnSn(SSe)_4$ (CZTSS).

In difference to CIGS, CZTS is based on non-toxic and abundantly available elements. The current record efficiency is 12%. It is achieved with an CZTSS solar cells on lab-scale by IBM [47].

13.4.2 Cadmium telluride solar cells

In this section we will discuss the *cadmium telluride* (CdTe) technology, which currently is the thin-film technology with the lowest demonstrated cost per W_p. We start with discussing the physical properties of CdTe, which is a II-VI semiconductor because it consists of the II valence electron element cadmium (Cd) and the VI valence electron element tellurium (Te). Like the III-V semiconductors discussed in Section 13.2, CdTe forms a *zincblende* lattice structure where every Cd atom is bonded to four Te atoms and vice versa.

The bandgap of CdTe is 1.44 eV, a value which is close to the optimal bandgap for single junction solar cell. CdTe is a direct bandgap material, consequently only a few micrometres of CdTe are required to absorb all the photons with an energy higher than the bandgap energy. If the light-excited charge carriers should be efficiently collected at the contacts, their diffusion coefficient has to be in the order of the thickness.

CdTe can be *n*-doped by replacing the II-valence electron atom Cd with a III-valence electron atom like aluminium, gallium or indium. *n*-doping can be achieved as well by replacing a VI-valence tellurium atom with a VII-valence electron element like fluorine, chlorine, bromine and iodine atoms. The III- and VII-valence atoms act as shallow donors. Also a tellurium vacancy acts like a donor.

p-doping of CdTe can be achieved by replacing Cd with a I-valence electron atom like copper, silver or gold. It can be achieved as well by replacing Te atoms with V-valence electron elements such as nitrogen, phosphorus or arsenic. These elements act as shallow acceptors. But also a Cd vacancy acts as an acceptor. In solar cells, *p*-doped CdTe is used. However, it is difficult to obtain CdTe with a high doping level.

Figure 13.22 (a) shows the structure of a typical CdTe solar cell. First, transparent front contact is deposited onto the glass superstrate. This can be *tin oxide* or *cadmium stannate*, which is a Cd-Sn-oxide alloy. On top of that the *n*-layer is deposited, which is a *cadmium sulphide* layer, similar to the *n*-buffer layer in CIGS solar cells (Section 13.4.1). Then, the *p*-type CdTe absorber layer is deposited with a typical thickness of a few micrometers.